



Flexible Thermoelectric Module Using Bi-Te and Sb-Te Thin Films for Temperature Sensors

SU HYEON LEE,¹ HAISHAN SHEN,^{1,2} and SEUNGWOO HAN ^{1,3}

1.—Department of Applied Nano-mechanics, Korea Institute of Machinery and Materials, 156 Gajeongbuk-Ro, Yuseong-Gu, Daejeon 34103, Republic of Korea. 2.—Department of Advanced Materials Science and Engineering, Sungkyunkwan University, 2066, Seou-ro, Jangan-gu, Suwon-si 440-746, Republic of Korea. 3.—e-mail: swan@kimm.re.kr

Electromotive force is generated by a temperature difference in a thermocouple formed of two different metals, known as the Seebeck effect. Flexible thermoelectric (TE) temperature sensors based on the Seebeck effect can be attached to the body to provide body temperature information to health providers via wireless communications. Materials used in flexible TE temperature sensors have higher Seebeck coefficients than those of traditional thermocouples, and hence generate a high output voltage even with small temperature changes, making them highly suitable for use as body temperature sensors. In this study, a flexible TE temperature sensor was fabricated using a cheap, commercial flexible printed circuit board substrate and TE thin films of *n*-type bismuth telluride and *p*-type antimony telluride by co-evaporation. The results show that the flexible TE temperature sensor has a sensitivity of 192.70 $\mu\text{V K}^{-1}$.

Key words: Temperature sensor, flexible thermoelectric devices, thermocouple, bismuth telluride, antimony telluride

INTRODUCTION

Recently, flexible thermoelectric (TE) modules have been developed for a range of applications including smart clothes, smart watches, biosensors and temperature sensors. Flexible TE modules can be bent and wrapped easily around curved surfaces; hence, they can be used to produce wearable medical sensors that can be provided over a patient's body, with wireless communications to form a wireless body area network (WBAN).^{1,2} Data obtained using such sensors are sent via Bluetooth and collected by a mobile phone, which in turn sends the patient information via the Internet to a health service provider for real-time monitoring.²

Thermocouples use the electromotive force, which is the voltage arising from a temperature difference between two dissimilar materials. This effect is called the Seebeck effect, and was discovered by

Thomas Johann Seebeck in 1821. The Seebeck coefficient, $S_{ab} = S_b - S_a$, for two dissimilar conducting materials is given by

$$S_{ab} = \lim_{\Delta T \rightarrow 0} \frac{\Delta V_{ab}}{\Delta T} \quad (1)$$

where ΔV_{ab} is the electric potential across the interface of the two dissimilar conductors within a thermal gradient, and ΔT is the temperature difference between the conductor materials.³ The temperature difference between the hot and cold ends of the TE elements create a voltage potential, the Seebeck voltage, which drives hole/electron flow.⁴

Traditional thermocouples are usually chromel–alumel (K-type), chromel–constantan (E-type), or copper–constantan (T-type).^{5,6} TE materials generally have a higher Seebeck coefficient than traditional thermocouple materials. Transforming the voltage generated by a thermocouple into an accurate temperature reading is not simple, because the output voltage of traditional thermocouples is small;

(Received November 29, 2018; accepted April 16, 2019; published online April 24, 2019)

it is therefore important to generate a high-output signal to avoid generation of noise through signal amplification.⁶ The sensitivity of thermocouples can be described by the size and speed of the generated voltage following a minimal temperature change, and is derived by plotting voltage versus temperature data. The slope of this plot gives the Seebeck coefficient. Thus, thermocouples with very large Seebeck coefficients are critical in applications that require very sensitive and accurate temperature measurements.⁷

In this study, we fabricated a flexible TE module containing bismuth telluride *n*-type and antimony telluride *p*-type on a flexible printed circuit board (FPCB). Cheap and flexible TE thin films were fabricated by co-evaporation; the FPCB was composed of polyimide (PI) film and copper foil. Electrodes were patterned on the PI films by wet etching. An output voltage-temperature difference curve was obtained for the TE module for the temperature range 0.38°C to 133°C to evaluate its performance as a temperature sensor.

EXPERIMENTAL DETAILS

Process for Flexible TE Module Fabrication

A TE temperature sensor was fabricated on a double-sided FPCB substrate by co-evaporation (Bi-Te, Sb-Te). Figure 1 shows the fabrication process for the flexible TE module. The thickness of the PI film was 25 μm , and the initial thickness of the copper was 12 μm (Fig. 1a). The FPCB was cut to a 4-inch wafer size. A bonded dry film photoresist (DFR) was prepared on the FPCB for electrode patterning by exposure and etching, through a photolithography process (Fig. 1b). Holes were drilled where the electrodes were formed. The thickness of the copper was increased around the electrodes to 18 μm by electroplating plated-through holes (PTH). The DFR was then removed (Fig. 1c). The DFR was patterned by photolithography to etch the copper, except around the top and

the bottom of the electrodes. The DFR was then removed (Fig. 1d and e). *n*-type Bi-Te legs were deposited by co-evaporation. A stainless-steel mask was used to produce the patterns. To promote adhesion between the FPCB substrate and the *n*-type TE thin film, chrome (Cr) was first deposited. A 99.999% pure Cr source (1561°C source temperature at deposition) was evaporated for 10 min 30 s at a substrate temperature of 200°C to produce a 60-nm thickness; then, high-purity (99.999%) Bi, Sb and Te sources were evaporated. Evaporation temperatures were 658°C and 270°C for the Bi and Te sources, respectively. The evaporation rates for Bi and Te were 1.3 \AA s^{-1} and 2.6 \AA s^{-1} , respectively. The evaporation was conducted under vacuum for 11 h 56 min, while maintaining a main chamber pressure of 1.3332×10^{-7} kPa at a 200°C substrate temperature to produce a thickness of 18.64 μm (Fig. 1f). After the *n*-type deposition, *p*-type Sb-Te was deposited using the same metal mask. Likewise, for better adhesion, Cr (1568°C source temperature at deposition) was deposited at a substrate temperature of 200°C for 9 min. After Cr deposition, Sb and Te were evaporated at source temperatures of 408°C and 296°C, respectively. The evaporation rates for Sb and Te were 1.5 \AA s^{-1} and 3.8 \AA s^{-1} , respectively. The evaporation was conducted for 11 h 22 min at a substrate temperature of 200°C to obtain a thickness of 38.449 μm (Fig. 1g). The patterned products were then cut with a cutter after covering in polydimethylsiloxane (PDMS) to retain a *p-n* junction for temperature sensor measurements (Fig. 1h).

Evaluation of Thermocouple Sensitivity and Bending Radius-Internal Resistivity Curves

The surface morphology of the TE thin films was measured by field emission-scanning electron microscopy (FE-SEM, SU8230; Hitachi Ltd., Tokyo, Japan) and the cross-sectional shape was examined using ultra-high-resolution scanning electron microscopy (UHR-SEM, MAGELLAN400' FEI, Thermo Fisher Scientific, Waltham, MA, USA). The composition ratio of the TE thin films was measured by energy-dispersive x-ray spectroscopy (EDS, X-MaxN; Oxford Instruments, Abingdon, UK). The Seebeck coefficient was obtained using a Fraunhofer-IPM system (Breisgau, Germany) capable of measuring the voltage at different temperatures. The resistance was determined using a sheet resistance measurement method and a Hall-effect measurement system (Ecopia HMS-5000; Four Point Probes/Bridge Technology, Chandler Heights, AZ, USA).

The TE *p-n* junction that was cut to form a flexible TE generator was placed halfway between a heater and a heat sink to obtain a temperature difference across the sample. Thermal pads for current insulation were installed on the heater,

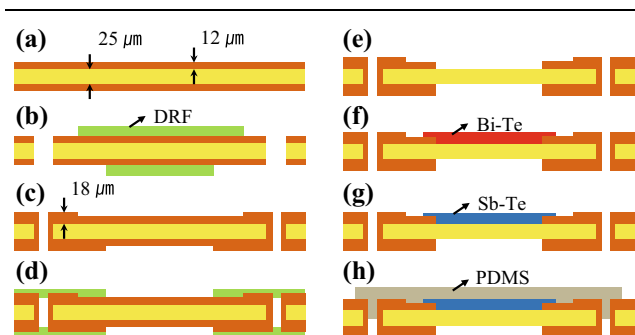


Fig. 1. Fabrication process of flexible thermoelectric (TE) module: (a) flexible printed circuit board (FPCB) cut to a 4-inch wafer size, (b) dry film photoresist (DFR) patterning and hole drilling, (c) Cu electroplating and removal of DFR, (d) DFR patterning, (e) Cu etching and DFR removal, (f) deposition of *n*-type Bi-Te thin film, (g) deposition of *p*-type Sb-Te thin film and (h) spin-coating of polydimethylsiloxane (PDMS) cover layer.

the heatsink, under the flexible TE module bottom electrodes, and between the upper electrodes and the copper blocks. Temperatures were measured at four points (heater, heat sink, hot-side and cold-side electrode on the TE module) using a K-type thermocouple, and the direct current (DC) voltage generated from the temperature difference was measured using a SourceMeter 2400 (Keithley Instruments, Cleveland, OH, USA) connected to electrodes and gold wiring. The open voltage was measured while the set temperature of the heater was increased from 23°C to 200°C. The experimental setup is shown in Fig. 2.

In addition, a bending radius-internal resistance curve was obtained by measuring the internal resistance of the flexible TE module using a SourceMeter 2400 (Keithley) under a range of tensile and compressive strain conditions. Figure 3 shows an image of the flexible TE module during measurement of the internal resistance at different curvature radii.

RESULTS AND DISCUSSION

Property and Characteristics of Thermoelectric Thin Films

Figure 4 shows the SEM surface and cross-sectional images of the TE thin films. Surface images of the *n*-type Bi-Te are shown in Fig. 4a and b, and a cross-sectional image is shown in Fig. 4c. A surface image of the *p*-type Sb-Te is shown in Fig. 4d, and a cross-sectional image is shown in Fig. 4f. The thicknesses of the *n*-type Bi-Te and *p*-type Sb-Te were 18.64 μm and 38.49 μm , respectively.

Table I provides performance parameters for the materials used in traditional thermocouples and the deposited Bi-Te and Sb-Te thin films. The Seebeck coefficients of the K-type, E-type and T-type thermocouple metals are $-18.30 \mu\text{V K}^{-1}$ (alumel), $22.20 \mu\text{V K}^{-1}$ (chromel), $-39.90 \mu\text{V K}^{-1}$ (constantan) and $1.94 \mu\text{V K}^{-1}$ (copper).⁵ The Seebeck coefficients of the Bi-Te and Sb-Te thin films fabricated in

this study were $-24.82 \mu\text{V K}^{-1}$ and $200.16 \mu\text{V K}^{-1}$, respectively. The Seebeck coefficient of the Bi-Te thin film is low because the atomic ratio of Te is not stoichiometric, with a composition ratio of 43 atomic weight percent (at.%) Bi and 57 at.% Te. Liao al.⁸ reported Seebeck coefficients, measured at room temperature, of the Bi/Te samples annealed at 200°C for 12 h as a function of Te atomic concentration. Goncalves et al.⁹ evaluated the Seebeck coefficient of Bi₂Te₃ thin films as a function of the Te/Bi evaporation flow rate ratio (*R*) for films deposited at different substrate temperatures (190°C, 230°C and 270°C) by thermal co-evaporation. They reported that Bi-Te thin films have a low Seebeck coefficient when Te is similar in content. It is therefore necessary to further investigate the potential for improvements in the TE properties of Bi-Te thin films, by adjusting the composition ratio. However, the composition ratio of the Sb-Te thin film was 36 at.% Sb and 64 at.% Te, with a Seebeck coefficient of $200.16 \mu\text{V K}^{-1}$. This is five times higher than the value of $-39.90 \mu\text{V K}^{-1}$ for constantan, which has the highest Seebeck coefficient among the materials used in conventional thermocouples. The Seebeck coefficient of Sb-Te thin film is high, even though the stoichiometry is not Sb₂Te₃. Ping et al. reported the Seebeck coefficient of the films versus the atomic ratio of Sb to Te; Te-rich films showed a higher Seebeck coefficient.¹⁰



Fig. 3. Images for the bending test of the flexible TE module.

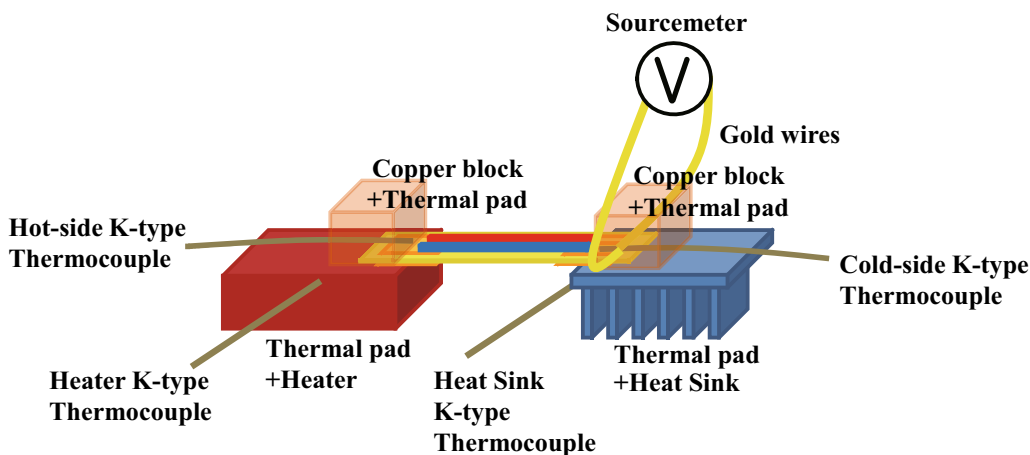


Fig. 2. Performance evaluation system for the flexible TE module.

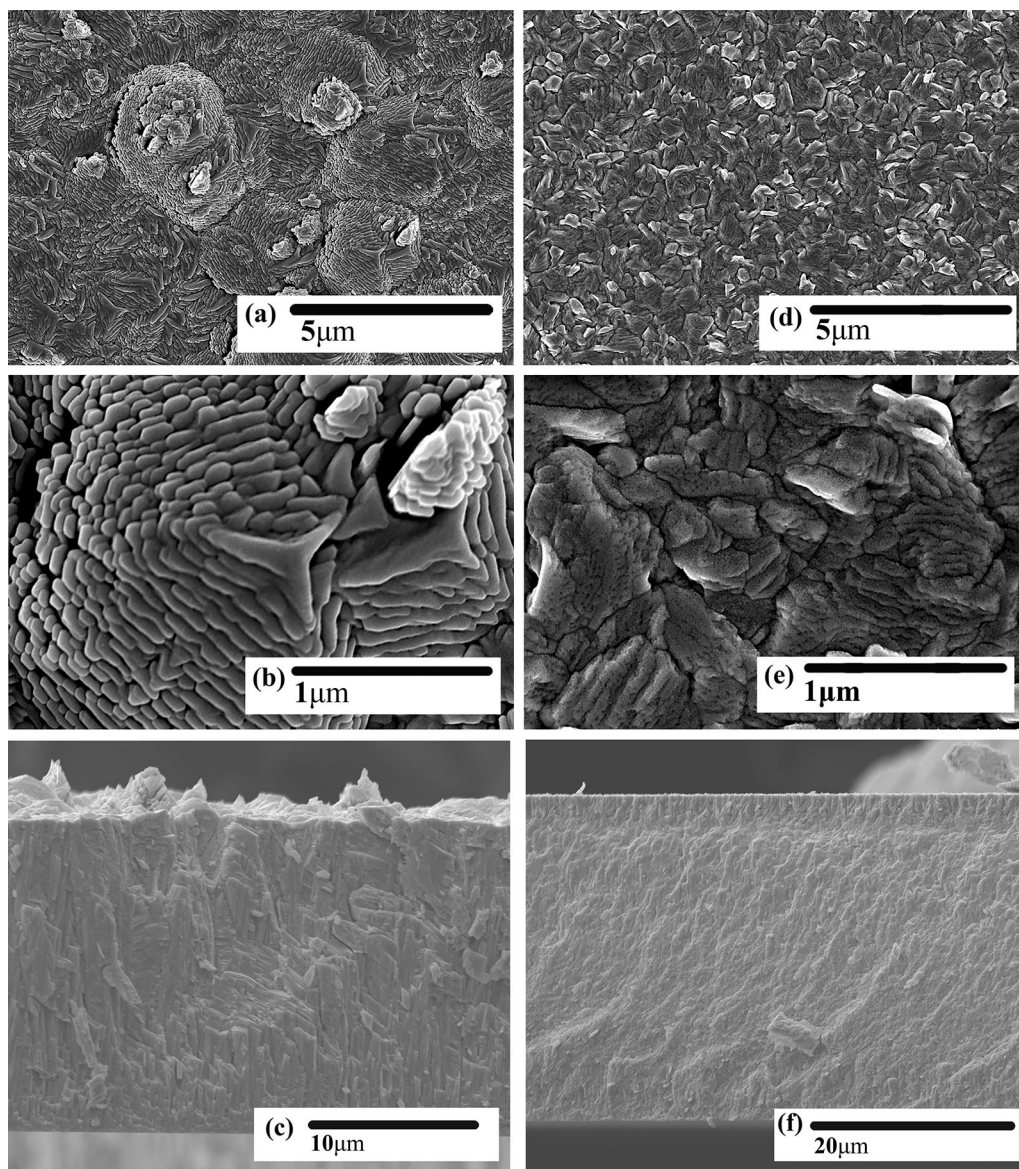


Fig. 4. SEM images showing surfaces and cross sections of the co-evaporated TE material thin films: (a), (b) top section of the *n*-type Bi-Te thin film; (c) cross section of the *n*-type Bi-Te thin film; (d), (e) top section of the *p*-type Sb-Te thin film; and (f) cross section of *p*-type Sb-Te thin film.

Table I. Properties of thermocouple materials and TE films

| Thermocouple type | Material | Composition (at.%) ⁵ | Thickness (μm) | Seebeck coefficient ($\mu\text{V K}^{-1}$) ⁷ |
|-------------------|-------------------------|---------------------------------|-----------------------------|---|
| K-type | Alumel (Ni-Mn-Al-Si) | 95-2-1-1 | Bulk | -18.30 |
| E-type | Chromel (Ni-Cr) | 90-10 | Bulk | 22.20 |
| T-type | Constantan (Cu-Ni) | 55-45 | Bulk | -39.90 |
| Ours | Cu | 100 | Bulk | 1.94 |
| | Bi-Te | 43-57 | 18.64 | -24.82 |
| | Sb-Te | 36-64 | 32.27 | 200.16 |

Sensitivity Characteristic and Internal Resistance with Respect to the Radius of Curvature of the Fabricated Flexible TE Temperature Sensor

Figure 5 shows images of the flexible TE device and a flexible TE temperature sensor fabricated by cutting out the *p-n* junction. There are two *p-n* junctions in each flexible TE device. For sensitivity measurements, the temperatures of the high- and low-temperature parts of the flexible TE element electrode were measured using a K-type thermocouple, because when measuring the characteristics of the flexible TE temperature sensor, the temperature measurements should simulate the actual situation of the TE thin film. Figure 6 shows the temperature of the high- and low-temperature electrodes of the flexible TE element measured using the K-type thermocouple, according to the temperature setting of the heater. As the set temperature of the heater increases, the temperature difference between the high- and low-temperature electrode of the element increases.

The thermal conductivity of the copper is $401 \text{ W m}^{-1} \text{ K}^{-1}$,¹¹ and that of the PI film is $0.46 \text{ W m}^{-1} \text{ K}^{-1}$.¹² Sufficient heat conduction did not reach the flexible TE thin film deposited on the FPCB substrate from the heat source applied to the flexible TE temperature sensor. Therefore, when designing the flexible TE device, the PTH technique was used to connect the top and bottom electrodes to improve heat conduction.

Figure 7 shows a schematic diagram of the heat flow between the electrodes in TE devices on PI film and the FPCB substrate using the PTH technique.

A graph of the output voltage with respect to the measured temperature difference is shown in Fig. 8. The output voltage of a conventional thermocouple was measured using a connection between the thermocouple material and a copper wire immersed in an ice bath to maintain the temperature difference.⁶

Table II shows the slopes and Pearson's ratio correlation coefficients obtained by fitting the graphs of the output voltage to the measured temperature difference, for temperature differences

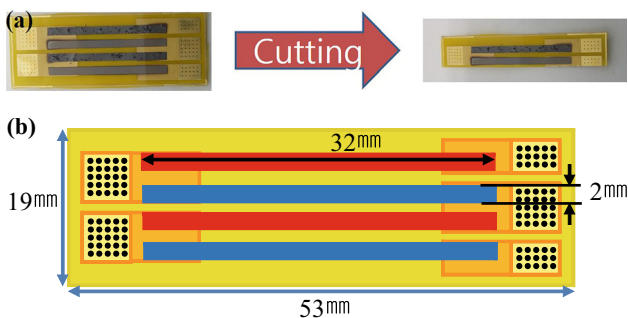


Fig. 5. Flexible TE device and flexible TE module: (a) pictures and (b) dimensions of the flexible TE device.

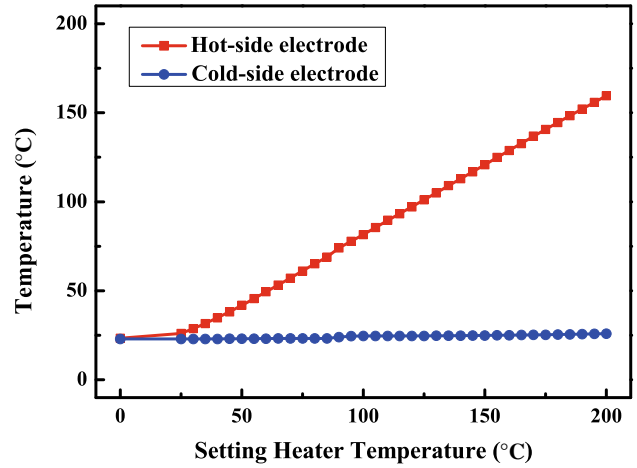


Fig. 6. Temperature differences between the hot-side and cold-side electrode.

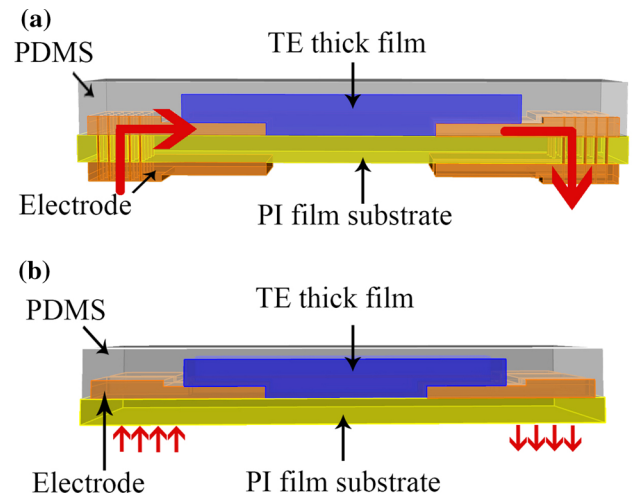


Fig. 7. Schematic diagrams of the embodied TE devices using PI film and FPCB substrates: (a) TE module on FPCB substrates using the PTH technique and (b) the TE module on PI film.

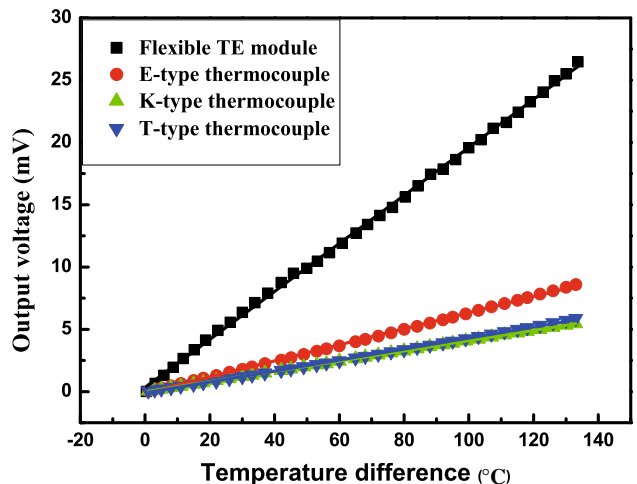


Fig. 8. Graph of the output voltage according to the temperature difference.

Table II. Fitting value of flexible TE module, E-type, K-type and T-type

| Type | Seebeck coefficient (mV/°C, at 0.38 ~ 133°C) | Pearson's r value |
|--------------------|--|---------------------|
| Flexible TE module | 0.1927 | 0.9996 |
| E-type | 0.0645 | 0.9997 |
| K-type | 0.0411 | 0.9999 |
| T-type | 0.0440 | 0.9994 |

between 0.38°C and 133°C. The slope represents the Seebeck coefficient. The value for the flexible TE module was 0.1927 mV/°C, about three times higher than that for the E-type at 0.0645 mV/°C and about four times higher than those of the K-type (0.0411 mV/°C) and T-type (0.0440 mV/°C).

The combined Seebeck coefficient constant, S , is given by

$$S = |S_n| + |S_p| \quad (2)$$

where S_n and S_p are the Seebeck coefficients of the n - and p -type semiconductors, respectively.¹³ According to Eq. 2, the Seebeck coefficient constant of the flexible TE module is 224.98 $\mu\text{V K}^{-1}$, about 14% lower than the measured value of 192.70 $\mu\text{V K}^{-1}$; this is due to the contact resistance between the electrode and the TE thin film.

A measure of the linear dependence between X and Y , that is two variables, is the Pearson correlation coefficient. It has a value between +1 and -1 inclusive, where 1 represents completely positive correlation, 0 is no correlation and -1 is a completely negative correlation. The r -value is +1 if X and Y are identical, 0 if they are completely different and -1 if X and Y are identical in value but opposite in sign.¹⁴ The Pearson correlation coefficients were 0.9996 (flexible TE module), 0.9997 (E-type), 0.9999 (K-type) and 0.9994 (T-type); hence, the fitted and measured values were nearly identical for all sets of measurements.

The flexible TE module was subjected to compressive stress and tensile stress along the direction of the bending plane, shown schematically in Fig. 9. In Fig. 9a, a portion of the deposited TE thin film was bent inward and compressive stress was applied; in contrast, in Fig. 9b, a portion of the deposited TE thin film was bent outward, and tensile stress was applied. Under tensile stress, the TE thin film cracked, leading to an increase in the internal resistance. Figure 10 shows the rate of change in internal resistance as a function of the curvature radius. When tensile stress was applied at curvature radii of 36 mm, 23 mm, 18 mm and 11 mm, the internal resistance increased by 3%, 8%, 15% and 27%, respectively. On the other hand, under compression stress, there was little to no change in the internal resistance as the radius of curvature decreased.

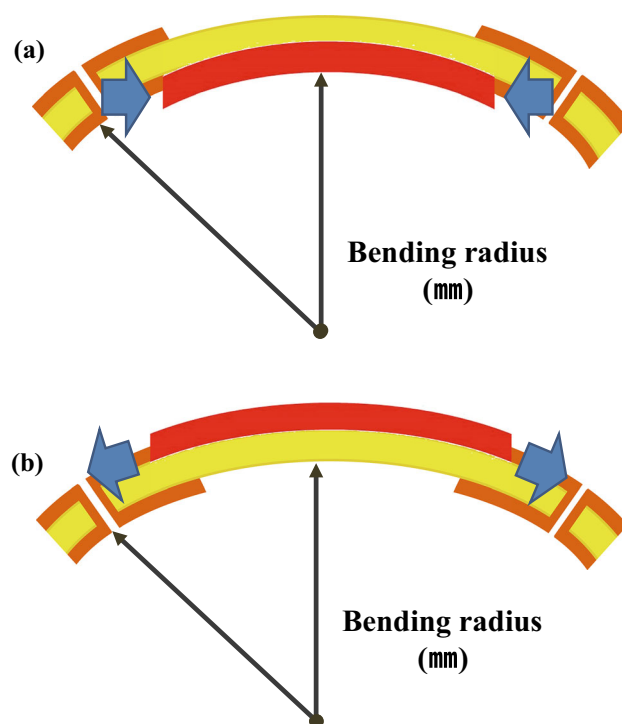


Fig. 9. Schematic diagrams of the production of bending-strained TE thin films: (a) TE module with applied compressive stress and (b) TE module with applied tensile stress.

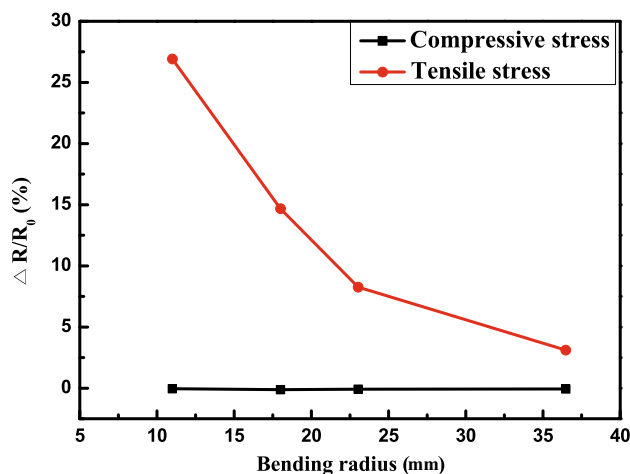


Fig. 10. Graph of internal resistance as a function of the curvature radius.

CONCLUSION

Flexible TE temperature sensors were fabricated by depositing *n*-type Bi-Te and *p*-type Sb-Te thin films on FPCB substrates. The fabricated flexible TE sensor had a Seebeck coefficient of 0.1927 mV/°C, about three times greater than an E-type thermocouple, and about four times greater than K-type and T-type thermocouples. When the flexible TE temperature sensor was subjected to compressive stress, there was no change in the internal resistance. The sensor can be applied to curved skin surfaces that have small temperature differences, and hence used for real-time monitoring of body temperatures.

Further study is necessary to improve the Seebeck coefficient of the *n*-type Bi-Te thin film by adjusting the composition ratio to 40 at.% Bi and 60 at.% Te. The Seebeck coefficient of *n*-type Bi-Te thin film was approximately $-200 \mu\text{V K}^{-1}$, similar to that of *p*-type Sb-Te thin film. The Seebeck coefficient of the flexible TE sensor could be increased further by $\sim 44\%$ by considering the effect of the contact resistance between the electrodes and the TE thin film.

ACKNOWLEDGMENTS

This work was supported by a National Research Foundation of Korea (NRF) grant funded by the Korean Government (MSIP) (NRF-2015R1A5A1036133)

REFERENCES

1. S. Ullah, H. Higgins, B. Braem, B. Latre, C. Blondia, I. Moerman, S. Saleem, Z. Rahman, and K.S. Kwak, *J. Med. Syst.* **36**, 1065–1094 (2012).
2. J.-H. Bahk, H. Fang, K. Yazawa, and A. Shakouri, *J. Mater. Chem. C* **3**, 10362–10374 (2015).
3. J. Martin, T. Tritt, and C. Uher, *J. Appl. Phys.* **1008**, 121101 (2010).
4. L.E. Bell, *Science* **321**, 1457–1461 (2008).
5. N. Auparay, in Bachelor Thesis, Department of Physics, Oregon State University, pp. 17–20 (2013).
6. M. Duff and J. Towey, Two ways to measure temperature using thermocouples feature simplicity, accuracy, and flexibility (Analog dialogue 44–10, October 2010). www.analog.com/analogdialogue. Accessed 15 March 2017.
7. M Jeong and S Han, *Sensor Mater.* **27**, 87–96 (2015).
8. C.-N. Liao and T.-H. She, *Thin Solid Films* **515**, 8059–8064 (2007).
9. L.M. Goncalves, C. Couto, P. Alpuim, A.G. Rolo, F. Völklein, and J.H. Correia, *Thin Solid Films* **518**, 2816–2821 (2010).
10. P. Fan, Z.-H. Zheng, G.-X. Liang, X.-M. Cai, and D.-P. Zhang, *Chin. Phys. Lett.* **27**, 087201 (2010).
11. Y.S. Touloukian, Thermal Conductivity-Metallic Elements and Alloys, vol. 1. (Thermophysical properties of matter 1970), pp. 66.
12. H Yokoyama, *Cryogenics* **35**, 799–800 (1995).
13. G. Ali, J. Wagner, D. Moline, and T. Schweisinger, *J. Renew. Energy* **74**, 528–535 (2015).
14. J.L. Rodgers and W.A. Nicewander, *Am. Stat.* **42**, 59–66 (1988).

Publisher's Note Springer Nature remains neutral with regard to jurisdictional claims in published maps and institutional affiliations.